VIP The following Communications have been judged by at least two referees to be "very important papers" and will be published online at www.angewandte.org soon:

Books

Highlights

Not just a pretty face: A new structural model for the [NiFe] hydrogenases (see structure, pale green Ni, dark green Ru, pink S, red H) is also functional: it activates H_2 to give a bimetallic hydride and H^+. This advance will encourage reinvestigation of the heterolysis of the implied H_2 adduct. Questions arise regarding Ni^{II} low-spin to high-spin interconversion and reclassification of [FeFe] versus [NiFe] hydrogenase models.

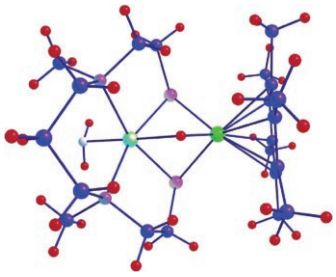

Hydrogenase Modeling

Molecular musclemen: Local stress from organic solid-state photoreactions may be released in a catastrophic manner, causing single crystals to fragment (see picture, bottom). Alternatively, crystals in topotactic reactions (see picture, top) release the stress by changing size and shape. These mechanical processes may be used to design photoactuators capable of performing work at the nano- to micrometer scales.

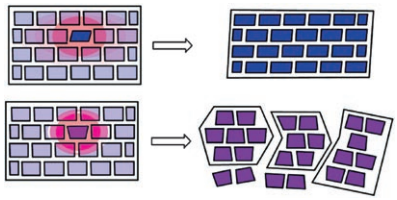

Crystalline Molecular Machines

Contents

Reviews

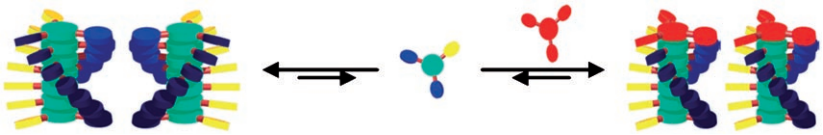

Origin of chirality: A subtle interplay of noncovalent interactions is necessary to observe the amplification of chirality in dynamic systems. Understanding why some systems amplify chirality may, ultimately, help answer the question as to how the molecules of life became homochiral. (The picture shows the sequence of fixing the chirality in a supramolecular aggregate.)

Communications

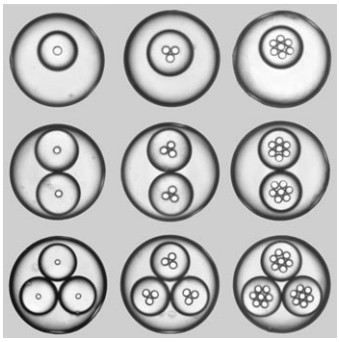

A drop within a drop within a drop: A microfluidic technique is used to generate highly controlled multiple emulsions (see picture). The high degree of control and scalability afforded by this method makes it a flexible and promising route for engineering designer emulsions and microcapsules with multiphase structures. Moreover, its generality will enable fabrication of novel materials containing complex internal structures.

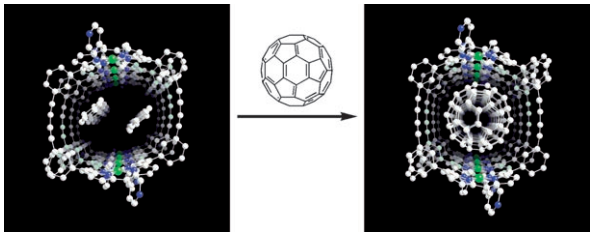

Like peas in a pod: X-ray crystallography reveals a self-assembled nanotube of cyclic porphyrin dimers and its inclusion complex with C_{60} (see picture, N blue, Ni green). The cyclic molecules stack through nonclassical C–H···N hydrogen bonds and π–π interactions of pyridyl groups to form the tubular structure. The C_{60} molecules are linearly arranged to form a supramolecular peapod.

For the USA and Canada:
ANGEWANDTE CHEMIE International Edition (ISSN 1433-7851) is published weekly by Wiley-VCH, PO Box 191161, 69451 Weinheim, Germany. Air freight and mailing in the USA by Publications Expediting Inc., 200 Meacham Ave., Elmont, NY 11003. Periodicals postage paid at Jamaica, NY 11431. US POSTMASTER: send address changes to *Angewandte Chemie*, Wiley-VCH, 111 River Street, Hoboken, NJ 07030. Annual subscription price for institutions: US$ 7225/6568 (valid for print and electronic / print or electronic delivery); for individuals who are personal members of a national chemical society prices are available on request. Postage and handling charges included. All prices are subject to local VAT/sales tax.

Reduce, reuse, recycle: Zwitterionic adducts of pyridyl-containing hexacoordinate phosphorus anions and $(C_5H_5)Ru$ moieties (see picture) are air-, moisture-, and microwave-stable catalysts that can be readily purified and in some instances recycled. Carroll rearrangements of allylic β-ketoesters performed with these species occur with improved regio- and enantioselectivity.

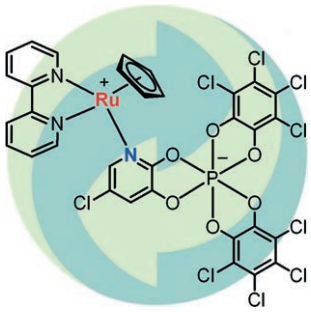

Homogeneous Catalysis

Changing faces: The shape of gold nanorods can be finely tuned by controlled growth under sonication in DMF in the presence of poly(vinylpyrrolidone). Reshaping involves the formation of rods with sharp tips and strongly faceted lateral faces, and ultimately leads to perfect, single-crystal octahedrons (see images). Mechanistic considerations indicate a shape-inducing effect of the polymer through different binding interactions for the different faces.

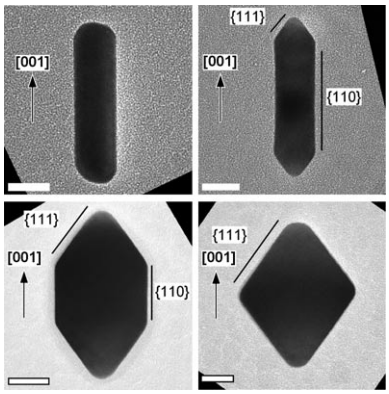

Gold Nanostructures

Getting rid of copper: A class of ternary Pt–Cu–Co electrocatalysts for the reduction of oxygen in polymer electrolyte membrane fuel cells shows unprecedented activity improvements over state-of-the-art Pt catalysts. The active phase of the catalysts is synthesized by selective electrochemical dissolution (dealloying, see picture) of Cu-rich alloy-particle precursors, resulting in Pt-enriched core–shell particles.

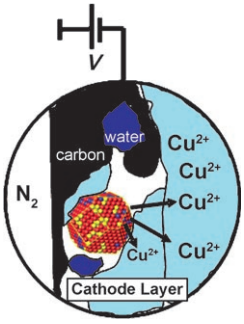

Electrocatalysis

Hydrogen first, oxygen next: The kinetics of water incorporation in situ has been followed by spatially resolved local optical absorption spectroscopy as well as by integral conductance by using $SrTiO_3$ as a model oxide proton conductor. The surprising nonmonotonic redox kinetics can be explained by a decoupling of the H_2O diffusion into a fast diffusion of hydrogen and a more sluggish diffusion of oxygen (see picture).

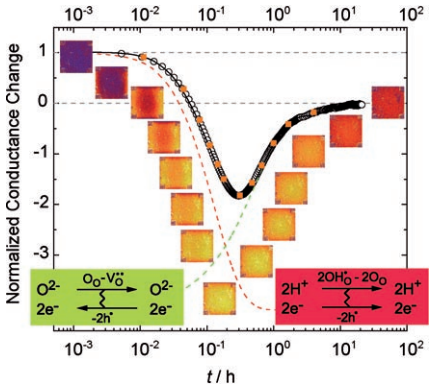

Water Incorporation

Incredibly selective!

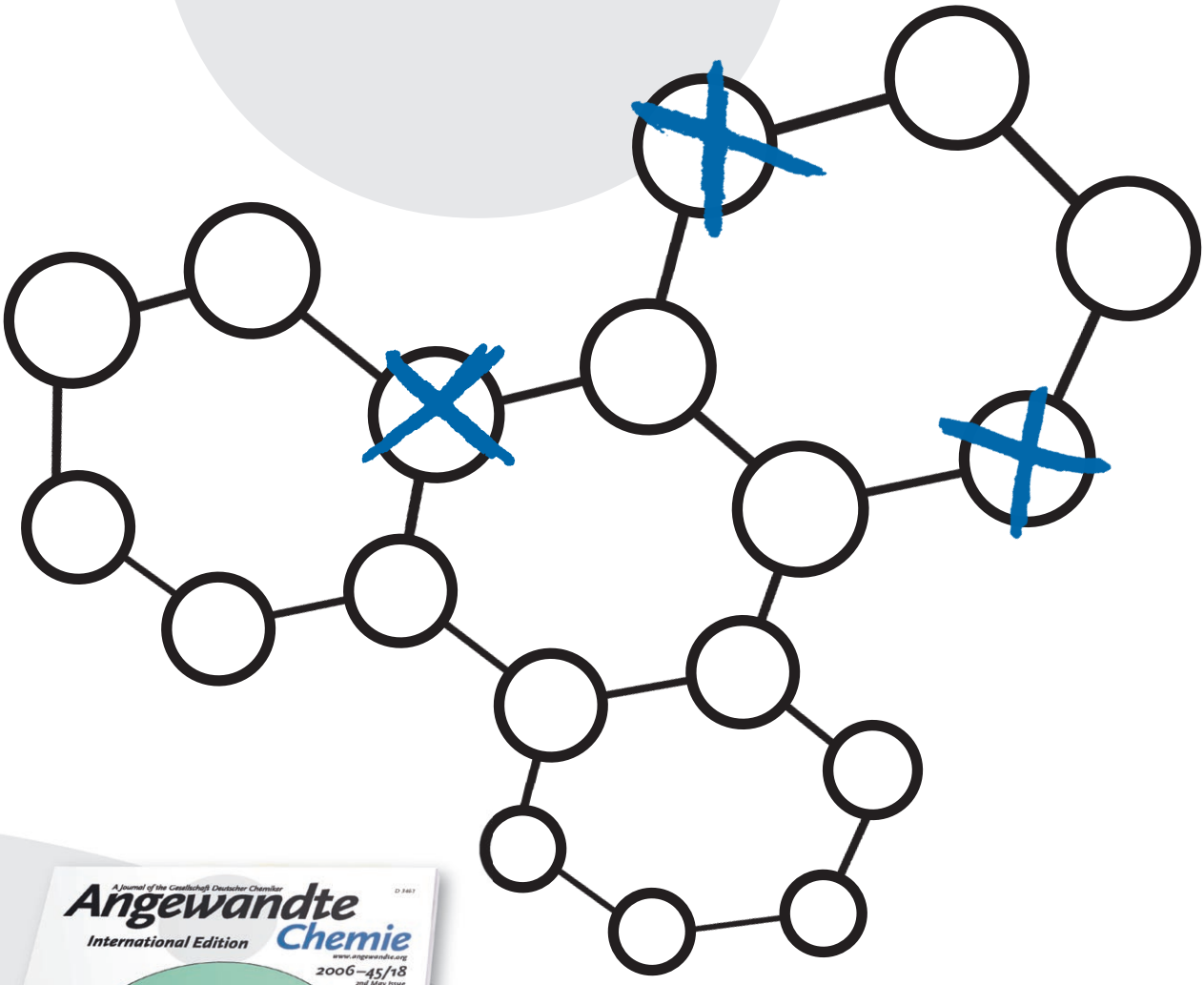

Angewandte Chemie chooses its articles carefully. Most of its Reviews, Highlights, and Essays are written upon invitation, from authors who are among the very best in their fields. Just 30 % of all submitted Communications in 2006 were accepted after peer review - only about 1400 from nearly 5000. Communications that are judged to be exceptionally important within a particular field are featured as Very Important Papers (VIPs).

GDCh Gesellschaft Deutscher Chemiker

BICENTENNIAL 1807 WILEY 2007 BICENTENNIAL

service@wiley-vch.de
www.angewandte.org

WILEY-VCH

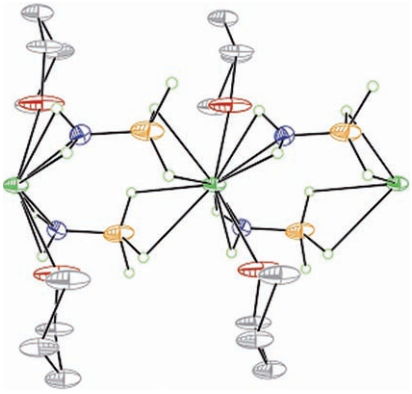

No foaming at the mouth here: A calcium(II) derivative of ammonia–borane, $Ca(NH_2BH_3)_2$ (see picture; green Ca, red O, blue N, yellow B, gray C, small green H), has thermal properties that are quite different from those of ammonia–borane. $Ca(NH_2BH_3)_2$ releases hydrogen over a temperature range of 100 to 170 °C without foaming.

Hydrogen Storage

Labeling diabetes: Streptozotocin-derived, cyanine-5.5-labeled imaging probes were synthesized and tested with the beta-cell-mimic INS-1E cell line in cell uptake assays, as well as by flow cytometry and confocal microscopy. Both probes showed superb labeling of INS-1E cells and human pancreatic islets (see graph) with no toxicity.

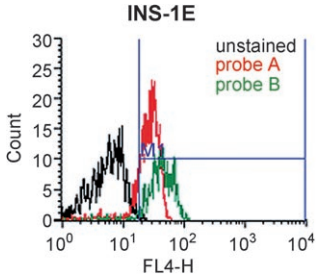

Fluorescent Probes

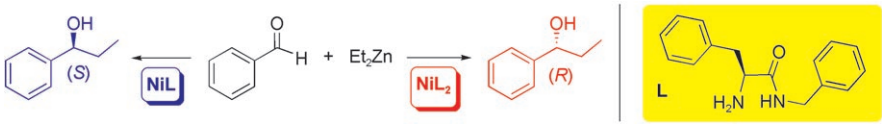

Asymmetric Catalysis

It works both ways: A very simple and efficient dual enantioselective control in the addition of diethylzinc to benzaldehyde can be achieved by using nickel complexes of chiral α-amino amide derivatives. Whereas complexes with 1:1 stoichiometries afford the *S* alcohol as the major enantiomer, 1:2 (metal/ligand) complexes lead to the predominant formation of the *R* enantiomer (see scheme).

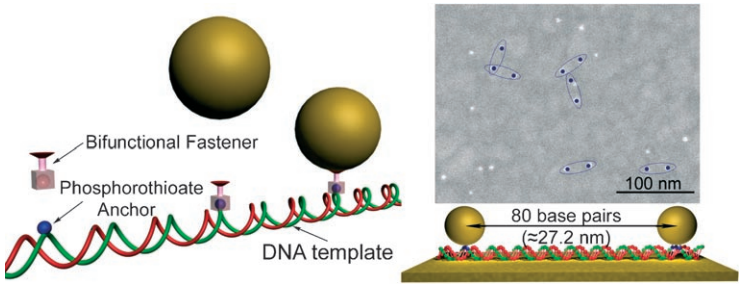

DNA Nanotechnology

Going for double gold: Precise control of the positions of and distances between gold nanoparticles (AuNP; gold spheres in picture) is achieved by linking the AuNPs to phosphorothioate-modified DNA (green and red helices) with a bifunctional fastener. The distance between AuNPs is controlled simply by changing the position of the modifications on the DNA template.

Contents

Go with the flow: The combination of phase-mask interference lithography and microfluidic flow lithography yields stop-flow interference lithography, a new route for the fabrication of large numbers of three-dimensionally patterned polymeric particles with sub-micrometer features. For example, two-sided Janus particles can be formed when streams of different photopolymerizable liquids are combined (see picture).

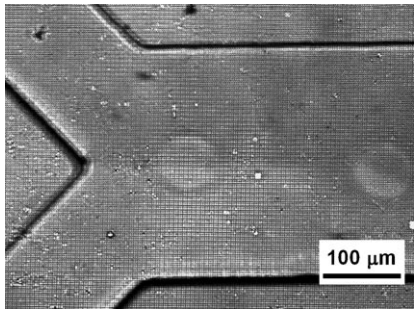

Lithography

Nd_3N pushes the limits: Unlike all the other encapsulated trimetallic nitride clusters (Sc_3N, Y_3N, Dy_3N, Gd_3N, ...), which prefer a C_{80} cage, the Nd_3N cluster is preferentially encapsulated in a larger C_{88} cage (see the HPLC trace in the picture). UV/Vis/NIR spectroscopy and electrochemistry performed on the isolated $Nd_3N@C_{88}$ fraction show a very small band gap for this compound.

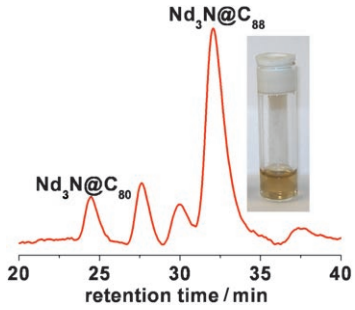

Endohedral Fullerenes

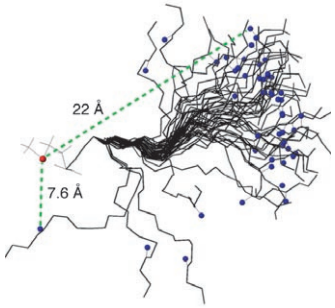

Local order goes with random coil: An ensemble of peptide structures is generated with over 90% extended conformation for Ala and Pro. The population-averaged long-range distance from the N-terminal spin-label residue (see picture, red dot) to the C-terminal amide proton of Ala (blue dots) is fully consistent with the results from NMR spin relaxation measurements.

Protein Folding

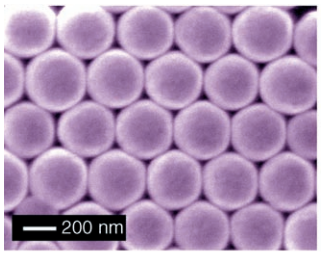

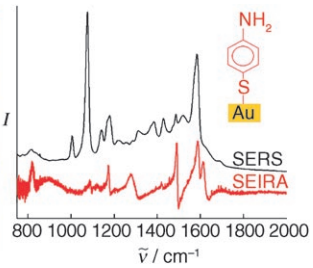

Sensitive support: Assembling plasmonic nanoshells into periodic arrays with nanoscale interparticle gaps gave a substrate on which surface-enhanced (SE) Raman spectroscopy (RS) and infrared absorption (IRA) spectroscopy can be performed simultaneously to enable molecular detection and characterization with high precision and sensitivity. The picture shows an SEM image of the Au nanoshell array and SERS and SEIRA spectra of a *p*-mercaptoaniline monolayer on the array.

Nanoshell Arrays

Contents

Going to the Mets: The uptake of Pt anticancer drugs also involves the Cu transporter Ctr1, which is located on the plasma membrane and contains functionally essential methionine-rich motifs. The methionine-rich peptide Mets7 reacts readily with Pt^{II} species. A striking difference between *cis*- and *trans*-$[PtCl_2(NH_3)_2]$ is that, upon reaction with Mets7, only the latter retains its N-donor ligands. Delivery of undegraded Pt drug to intracellular organelles by vesicle trafficking is hypothesized.

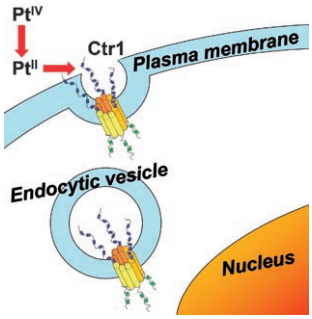

Anticancer Agents

Cl prevents insertion: The first metallanaphthalyne **2** has been obtained by Zn reduction of Os carbyne complex **1**. The key to its isolation was the use of *o*-chlorophenyl instead of phenyl substituents to avoid formation of a putative hydrido metallanaphthalyne intermediate (supported by DFT calculations), which undergoes migratory insertion of the carbyne into the Os–H bond and rearrangement to give an indenyl complex as the final product.

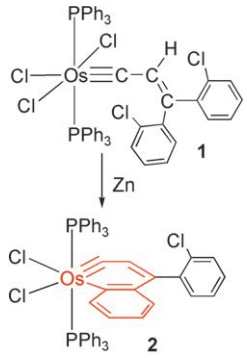

Metallaarenes

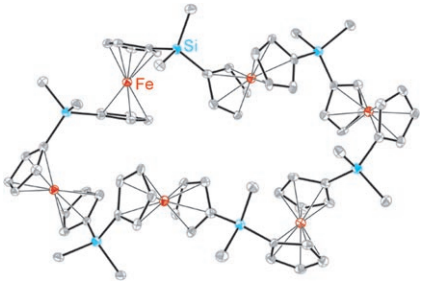

Coming full circle: Cyclic ferrocenylsilane oligomers (see structure) and polymers were prepared by the photolytic ring opening of a silicon-bridged [1]ferrocenophane with a bipyridine initiator. The relative amounts of cyclic oligomers and cyclic polymer, as well as the molecular weight of the cyclic polymer, can be controlled by the reaction temperature.

Organometallic Macrocycles

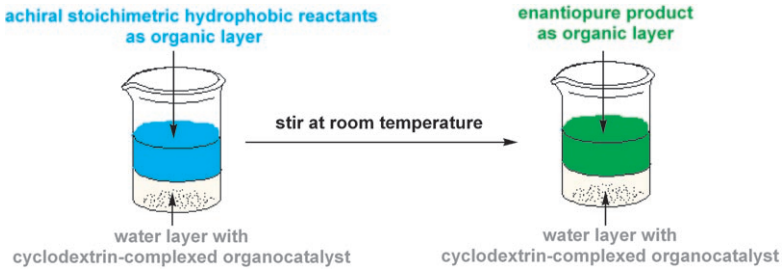

Hydrophobic pocket pleaser: A novel asymmetric catalytic system in water mediated by sulfated β-cyclodextrin (see picture) can bind the organocatalyst *tert*-butylphenoxyproline and associated hydrophobic reactants. Enantio- and diastereoselectivities up to >99% and close to quantitative yields could be achieved for stoichiometric direct aldol reactions of cyclohexanone and aryl aldehydes with this system.

Asymmetric Synthesis

Contents

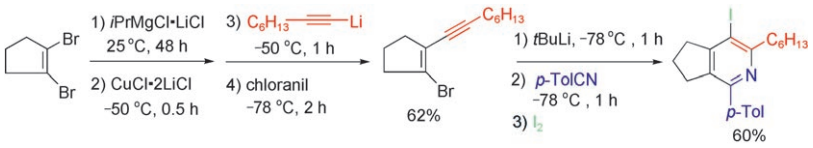

Oxidative Coupling

All crossed: The reaction of unsaturated copper reagents with various alkynyl lithium compounds provides mixed lithium cuprates, which in the presence of chloranil undergo an oxidative coupling, thus leading to polyfunctional alkynes or enynes. Bromoenynes prepared by this method are readily converted into pyridine derivatives by a new ring closure that proceeds at low temperature (see scheme, tol = tolyl).

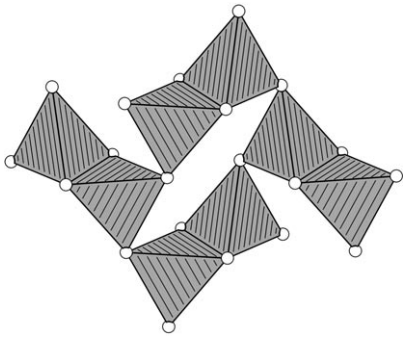

High-Pressure Borates

Going to extremes: A high-pressure borate was obtained under extreme conditions. In this species, each BO_4 tetrahedron is connected to a second BO_4 tetrahedron through a common edge (see structure).

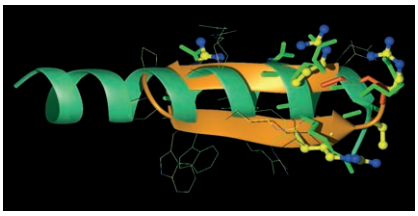

HIV Inhibitors

Bound to please: Binding of the Rev protein to HIV-1 RRE RNA is essential for virus replication. A strategy for the discovery of Rev-RRE inhibitors, based on the use of protein epitope mimetics, is described. Template-bound β-hairpin peptidomimetics (see picture, orange) are designed that mimic the Rev helical epitope (green). The mimetics bind with high affinity and selectivity to the target RNA, and have potential for development into novel anti-viral drugs.

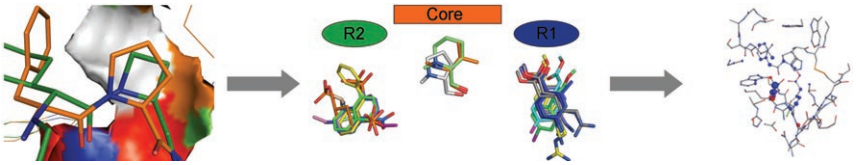

Drug Design

Divide and combine: KNOwledge Based Ligand Enumeration (KNOBLE) is a strategy for the design and synthesis of focused combinatorial libraries. This approach is based on the assembly of potential leads from fragments that are detected by the Cavbase subcavity matching algorithm comparing data from known crystal structures.

Contents

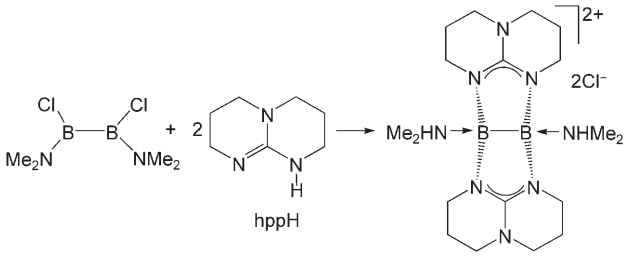

Bor-muda triangle: The first representative of a new type of boron cation is formed as the product of the reaction between $B_2Cl_2(NMe_2)_2$ and the guanidine derivative hppH (see scheme). The B–B bond length is typical for a single bond, and both boron atoms and the hpp nitrogen atoms bound directly to them form a trigonal prism.

Supporting information is available on the WWW (see article for access details).

A video clip is available as Supporting Information on the WWW (see article for access details).

Service

Corrigendum

A numerical error in Table 1 and Figure 3 has been brought to the attention of the authors of this Communication. The correct versions are provided below. Two corrections are also made to the figures in the Supporting Information. The authors apologize for the oversight, but note that the conclusions of the manuscript are not affected by these corrections.

Table 1: The parameters of the Eckart potential for the tunneling barrier to H_2 migration.

Cage, orientation[a]	E_0 [kcal mol^{-1}]	l [Å]	ν_s [10^{12} s^{-1}]
H_2 in small cage, $\perp$	23.687	3.30	15.024
H_2 in small cage, $\parallel$	28.414	3.14	17.246
H_2 in large cage, $\perp$	5.758	3.35	7.291
H_2 in large cage, $\parallel$	6.533	4.17	6.248

[a] See Figure 1.

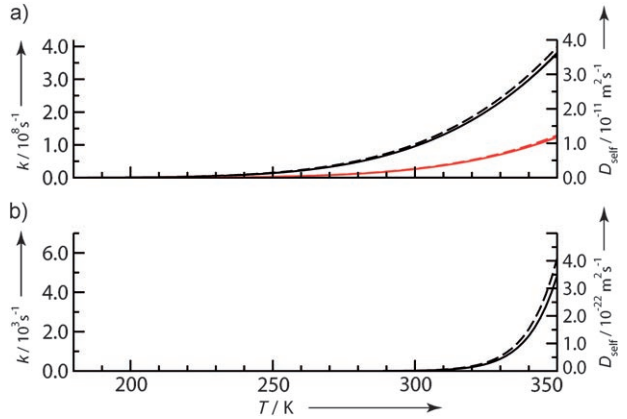

Figure 3. The rate of H_2 migration (k; left axis) and self-diffusion coefficient (D_{self}; right axis) through the cages of the sII chathrate hydrate as function of temperature: a) for an H_2 molecule oriented perpendicular (black: without tunneling, dashed black: with tunneling) and parallel (red: without tunneling, dashed red: with tunneling) to a hexagonal face of the large cage; b) for an H_2 molecule oriented perpendicular (black: without tunneling, dashed black: with tunneling) to a pentagonal face of the small cage (see Figure 1)

Hydrogen-Gas Migration through Clathrate Hydrate Cages

S. Alavi,* J. A. Ripmeester — **6102–6105**

Angew. Chem. Int. Ed. **2007**, *46*

DOI 10.1002/anie.200700250

